Crosslinkable sulfonated poly (diallyl-bisphenol ether ether ketone) membranes for vanadium redox flow battery application

Hongzhang Zhang [a,b], Huamin Zhang [a,*], Xianfeng Li [a,**], Zhensheng Mai [a,b], Wenping Wei [a,b], Yun Li [a,b]

[a] Division of energy storage, Dalian Institute of Chemical Physics, Chinese Academy of Sciences, Dalian 116023, China
[b] Graduate University of the Chinese Academy of Sciences, Beijing 100039, China

HIGHLIGHTS

► Crosslinkable SDPEEK membranes were prepared for VFB application.
► VFBs assembled with SDPEEK membranes show better performance than that of Nafion 115.
► The ion selectivity of SDPEEK membranes improved dramatically after UV crosslinking.
► The SDPEEK membranes keep stable after 900 h charge–discharge test.

ARTICLE INFO

ABSTRACT

Crosslinkable sulfonated poly (diallyl-bisphenol ether ether ketone) (SDPEEK) membranes with different degrees of sulfonation (DS) are prepared and first investigated in vanadium redox flow battery (VFB) application. The SDPEEK membranes with DS of 80% (SD4-6-100) show over an order of magnitude lower permeability of VO^{2+} ions (2.4×10^{-8} vs. 1.04×10^{-6} cm^2 min^{-1}) than currently used Nafion 115. The VFB battery assembled with SD4-6-100 membrane exhibits much higher columbic efficiency (98% vs. 92% at 50 mA cm^{-2}) and longer self-discharge time (180 h vs. 50 h) than that of Nafion 115, however, at similar energy efficiency. The membrane keeps a stable performance after 900 h charge–discharge test. In order to further improve the ions selectivity of SDPEEK membranes with high DS, the SD5-5-50 (DS 100%) membrane is crosslinked under ultraviolet (UV) radiation. The ion selectivity of the membrane is improved obviously after crosslinking, as a result, showing much higher columbic efficiency and energy efficiency.

1. Introduction

Renewable energies from sources like solar and wind are among the central topics of our times with the concerns of energy shortage and environment protection [1]. However, the random nature of these intermittent renewable sources (change with synoptic conditions, day and night alternation, etc.) makes it quite challenging for its use and dispatch through the grid [2]. One effective solution is to connect the power station and the grid with electrical energy storage devices. Vanadium redox flow battery (VFB) as one kind of energy storage techniques is rather suitable for this application due to its features like long life time, active thermal management as well as the independence of energy and power ratings [3–12].

As the key components of VFB system, the ion exchange membranes (IEMs) are employed to prevent the crossmixing of active species and transfer ions from anode to cathode or vice versa [13]. The ideal IEMs are supposed to own features like good ion conductivity, high ion selectivity, excellent chemical and mechanical stability, as well as low cost [14]. The membranes traditionally used in VFB are perflurosulfonic polymers such as DuPont Nafion® 115 or Nafion® 117. Even though the Nafion® membranes show both high proton conductivity and chemical stability, the extremely high cost and low ion selectivity of these membranes (high vanadium crossover) have limited the commercialization of VFB [15–17]. Other types of commercial membranes, such as anionic Selcmion AMV, DMV cationic Selemion CMV and micro-porous Daramic, were proved to be unsuitable in VFB application due to their low ion selectivity or poor chemical stability [16–20]. Thus, urgent need

* Corresponding author. Tel.: +86 411 84379072; fax: +86 411 84665057.
** Corresponding author. Tel.: +86 411 84379669; fax: +86 411 84665057.
E-mail addresses: zhanghm@dicp.ac.cn (H. Zhang), lixianfeng@dicp.ac.cn (X. Li).

was brought to develop substitute membranes for VFB application [21–23].

Recently, sulfonated or quaternized aromatic polymers like poly (arylene ether ketone) (PAEK), poly (arylene ether sulfone) (PES), polysulfone (PSF) and polyimide (PI), were widely reported for fuels cells application and gas separation due to their excellent thermal and mechanical stability. However, their application in VFB system is just started and only several kinds of poly aromatic polymers are investigated, like the quaternized or sulfonated poly (arylene ether ketone) [14,24–26], the sulfonated poly (arlene thioether) [27–30], the sulfonated polysulfone [31] etc. Although the VFBs assembled with these membranes show good battery efficiency, their chemical and mechanical stability still needs further improvement for commercial application [10,32].

Among most modification methods, crosslinking was proved to be one of the most efficient ways to improve the chemical and mechanical stability of membranes. The crosslinking usually can reinforce the polymers by forming networks between polymer chains and could also reduce the attacks from oxidant by suppressing the membrane swelling. In this paper, a series of crosslinkable sulfonated poly (diallyl-bisphenol ether ether ketone) (SDPEEK) were designed by introducing crosslinkable diallyl bisphenol A group onto the main chain of sulfonated poly (ether ether ketone) (SPEEK). For the first time, the SDPEEK membranes with different degrees of sulfonation (DS) were prepared and crosslinked with UV radiation for VFB application. The single cell performances assembled with these membranes were studied in detail.

2. Experimental

2.1. Polymer synthesis

The synthesis and characterization of SDPEEK polymers with different DS were described in previous article [33]. The DS of SDPEEK was adjusted via changing the content of sulfonated monomer. The structure of the polymer is shown in Fig. 1.

2.2. Membrane preparation

The polymer was first dissolved in N-methyl pyrrolidone (NMP) to form a 5–10 wt.% solution. The solution was then cast onto a clean glass plate and dried at 70 °C for 12 h. Afterward the membrane was peeled off and transformed to acid form by soaking into 0.5 M sulfur acid for 24 h.

As shown in Scheme 1, the crosslinked membrane was prepared by ultraviolet spectrum (UV) radiating (100 mW cm^{-2}, 125 W mercury lamp, 315 nm–410 nm) for 1.5-h with benzophenone and triethanolamine as the initiator according to Zhong et al. [34]. The detailed information of these membranes with different compositions was shown in Table 1.

2.3. Membrane characterization

2.3.1. Nuclear magnetic resonance (NMR) and Fourier transform infrared spectroscopy (FTIR)

NMR and FTIR were used to determine the chemical composition of the polymers. The ^{1}H NMR spectra were carried out on a BRUKER DRX400 spectrometer with deuterated dimethyl sulfoxide (DMSO-d_6) as the solvent and tetramethylsilane (TMS) as the internal standard. The IR spectra were recorded by using the ATR (attenuated total reflection) technique with an FTIR spectrometer (Avatar.370 E.S.P., Nicolet Continuum Infrared Microscope).

2.3.2. Thermogravimetric (TGA)

TGA analysis was obtained on a Pyris-diamond TG-DTA-THERMOSTER. Before test, all the polymers were preheated to 120 °C and kept at this temperature for 30 min to remove any residual moisture and solvent. After that, the temperature was heated to 700 °C with a heating rate of 5 °C min^{-1} under nitrogen flow.

2.3.3. Ion exchange capacity (IEC)

IEC was determined by the typical titration method. Membranes in acid form were first immersed in 1 M NaCl solution for 24 h to exchange all fixed H$^+$ ions of the membranes into the solution. Afterwards, the H$^+$ concentration in the solution was titrated with 0.01 M NaOH. And the IEC can be calculated by Eq. (1):

$$IEC = \frac{(C \times V)}{m} \tag{1}$$

where C and V were the concentration and the volume of NaOH solution, and m was the dried weight of the membranes.

2.3.4. Area resistance

The area resistance of the membranes was measured with the method described elsewhere [14]. A conductivity cell was separated into two compartments filled with 0.5 M H$_2$SO$_4$. The effective area of the cell (S) was 3 cm^2. r_1 and r_2, which represent the electric resistance of the cell with and without a membrane respectively, were determined by electrochemical impedance spectroscopy (EIS)
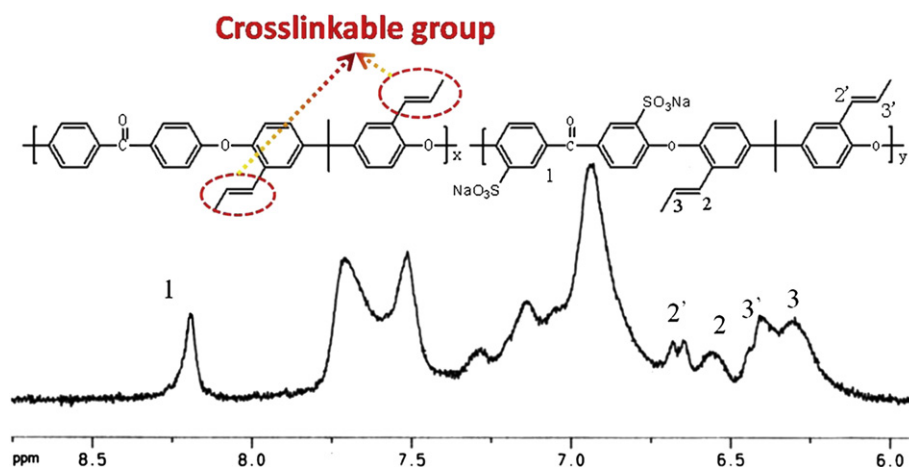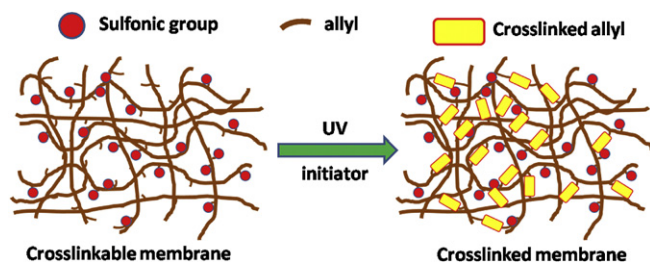

Fig. 1. The molecular structure and ^{1}H-NMR spectra of SDPEEK.

Scheme 1. The crosslinking mechanism of SDPEEK membranes with UV radiation.

over a frequency range from 100 kHz to 100 mHz. The area resistance r was calculated by Eq. (2):

$$r = (r_1 - r_2) \times S \tag{2}$$

2.3.5. Water uptake

The water uptake of the membranes was determined by traditional method reported previously [14]. The dried membranes were immersed in deionized water for 24 h at 25 °C. After quickly wiping out the surface water of the membranes, the weight of membrane was measured. The water uptake can be calculated based on the weight difference between the dried and swollen membranes (Eq. (3)).

$$\text{Water uptake} = \frac{W_{wet} - W_{dry}}{W_{dry}} \times 100\% \tag{3}$$

2.3.6. Vanadium permeability

The permeability of vanadium through the membranes was determined according to literature [20]. The diffusion cells are shown in Scheme 2. The left cell was filled with 1.5 M VOSO$_4$ in 3 M H$_2$SO$_4$ aqueous solution (60 ml) while the right one was filled with 1.5 M MgSO$_4$ in 3 M H$_2$SO$_4$ aqueous solution (60 ml) to equalize the ionic strengths and minimize the osmotic pressure effect. Solution in both cells was vigorously stirred to avoid the concentration polarization. The effective area of the membranes was 9 cm^2. Samples of 3 ml solution from the right cell were collected every 12 h. Subsequently another 3 ml fresh solution was added to the right cell to keep the solution volume stable. The vanadium concentration of samples was detected with UV–vis spectrometer. The vanadium permeability was determined according to the Fick diffusion law.

2.3.7. Scanning electronic microscopy (SEM)

SEM (JEOL-6360LV, Japan) was employed to observe the surface and cross-section morphology of the SD4-6-100 membrane before and after VFB cycle test. The cross-section of the membrane was obtained by breaking the membranes in liquid nitrogen and coating with gold particles.
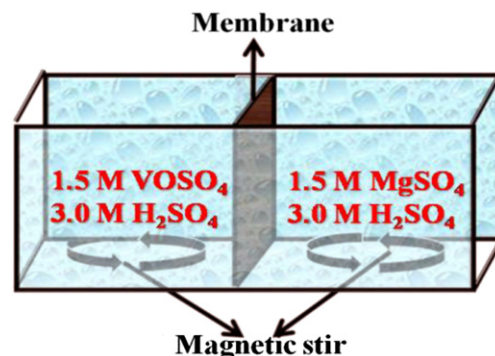
Scheme 2. The diffusion cells for vanadium permeability test.

2.3.8. VFB single cell performance

The VFB single cell was fabricated by sandwiching a membrane with two carbon felt electrodes, clamped by two graphite polar plates. All these components were fixed between two stainless plates. 30 ml 1.5 M V^{2+}/V^{3+} (1:1 mol) in 3.0 M H$_2$SO$_4$ (aq.) and 30 ml 1.5 M VO^{2+}/VO$_2^+$ (1:1 mol) in 3.0 M H$_2$SO$_4$ (aq.) were used as negative and positive electrolytes respectively. The electrolyte was cyclically pumped through the corresponding electrodes via airtight pipe lines. Charge–discharge cycling tests were conducted by LAND CT2001A and Arbin BT2000 with a constant current density of 50 mA cm^{-2}. The cut-off voltage for charge and discharge was set between 1.65 V and 0.8 V respectively to avoid the corrosion of carbon felt and graphite polar plates.

2.3.9. Self-discharge test

The VFB battery was assembled as mentioned in 2.3.8. Self-discharge started at the state of charge (SOC) of 50% and stopped until the voltage dropped below 0.8 V.

2.3.10. Cycling life test for VFB

The battery with SD4-6-100 was assembled as mentioned in 2.3.8. The cycling life test was operated under current density of 80 mA cm^{-2}.

3. Results and discussion

3.1. Polymer preparation and characterization

Fig. 2 shows the FTIR spectra of SDPEEKs with different DS. The absorption bands at 1027 and 1079 cm^{-1} are attributed to the symmetric and asymmetric O=S=O stretching vibrations of sodium sulfonated groups respectively. The area of these two characteristic peaks increases with DS. The peak at 965 cm^{-1} can be assigned to the group of allyl [28,29]. Peaks of ^{1}H-NMR spectra from 6.0 to 8.5 ppm correspond to the chemical shift of protons attaching to the aromatic rings (Fig. 1). The signal at 8.2 ppm is assigned to the aromatic hydrogen (H^1) ortho to the sulfonated groups. The DS of

Table 1
Physiochemical properties of SDPEEK and crosslinked SDPEEK membranes.

Membrane	Thickness (μm)	[a] Calculated DS (%)	Theoretical DS (%)	IEC (mequiv. g^{-1})	VO^{2+} Permeability ($\times 10^{-6}$ cm^2 h^{-1})	Water uptake (%)	CE (%)	VE (%)	EE (%)
SD3-7-100	100 ($\pm$5)	61	60	1.03	4.4	26.3	**96.7**	**88.9**	**86**
SD4-6-100	100 ($\pm$5)	76	80	1.2	2.3	42.5	**97.8**	**89.9**	**87.9**
SD5-5-100	100 ($\pm$5)	107	100	1.68	79.2	48.9	**94.5**	**89.4**	**84**
Nafion 115	125 ($\pm$3)	–	–	0.91	83.8	26.1	**91.3**	**91.9**	**84**
SD5-5-50	50 ($\pm$5)	107	100	1.64	41.2	49.0	**91.5**	**94**	**86**
C-SD5-5-50	50 ($\pm$5)	107	100	1.65	2.85	29.8	**97**	**93.1**	**90**

[a] DS based on ^{1}H NMR integration calculation.
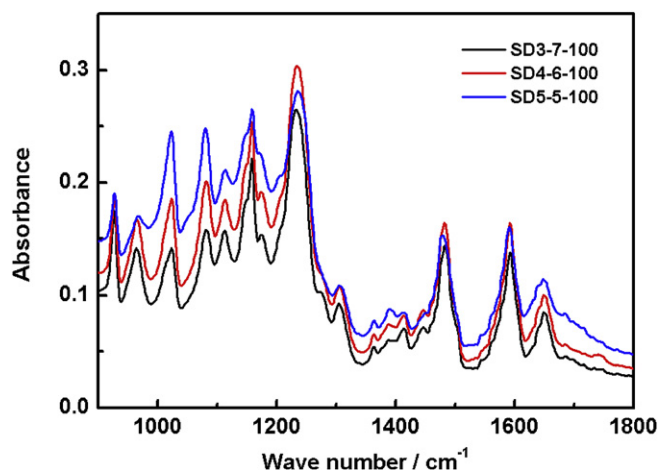
Fig. 2. The FTIR spectra of SDPEEK membranes.

Fig. 4. Area resistance of SDPEEK membranes in 0.5 M sulfuric acid.

the polymer can be calculated by Eq. (4) according to the ^{1}H NMR data.

$$\frac{\text{DS}}{14 - \text{DS}} = \frac{A_{H_1}}{\sum A_H} \tag{4}$$

where A_{H_1} is the peak area of H_1, $\sum A_H$ is the integral peak area of all aromatic hydrogen. As shown in Table 1, the DS determined by ^{1}H NMR is well consistent with the calculated value.

Fig. 3 shows the TGA curves of the SDPEEK membranes from 100 °C to 800 °C. The first weight loss stage occurring at around 300 °C is attributed to the splitting off of the sulfuric acid groups. The second degradation step starting at around 420 °C corresponds to the decomposition of the main chain. The TGA curve clearly indicates the excellent thermal stability of prepared SDPEEK membranes.

3.2. DS, water uptake and area resistance

As listed in Table 1 and Fig. 4, the water uptake of SDPEEK membranes increases obviously over the range of DS from 0.6 to 1.0, which is caused by the strong hydrophilicity of sulfonated group. Moreover, the area resistance decreases from 0.71 Ω cm^2 to 0.25 Ω cm^2 accordingly. Normally, the conductivity of these
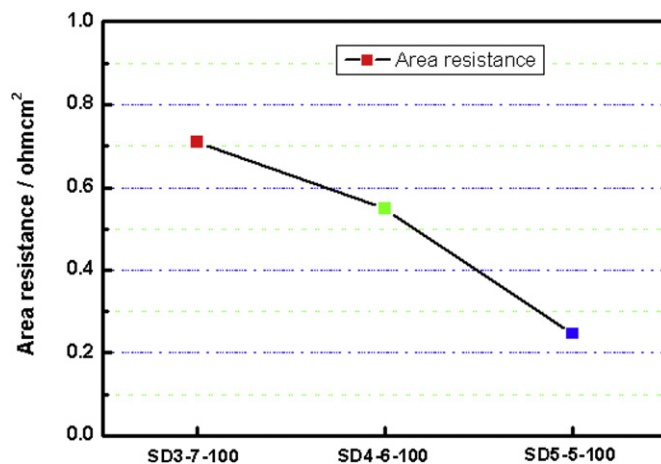
sulfonated membranes is mainly determined by DS and enhanced by the free water content inside the ion clusters of membranes. However the ion selectivity and membrane strength might be affected by ultrahigh water uptake, due to the high swelling of the membranes. In order to suppress the membrane swelling, the membrane with DS 100% was crosslinked with UV radiation. As a result, the water uptake of crosslinked membrane decreased by almost a half as shown in Table 1.

3.3. Vanadium permeability

The relationship between VO^{2+} concentration and diffusion time is illustrated in Fig. 5. As shown, the VO^{2+} diffusion rate increased obviously with membrane thickness from SD5-5-100 to SD5-5-50 and dropped sharply to C-SD5-5-50 after UV crosslinking. This phenomenon confirmed the supposition that the VO^{2+} permeation could be efficiently confined through crosslinking. And the VO^{2+} diffusion rate through the Nafion 115 membrane is much faster than through all the SDPEEK membranes, although the IEC of Nafion 115 membrane is comparatively much lower. This difference probably due to that the ions pathway of Nafion series membranes is more continuous than that of sulfonated hydrocarbon membranes [35].
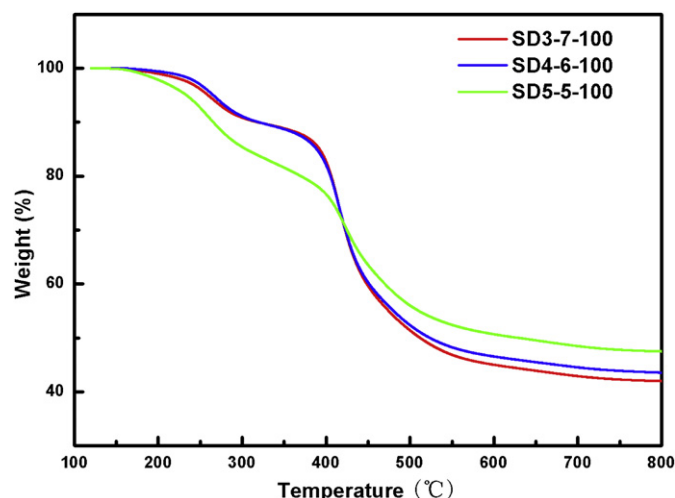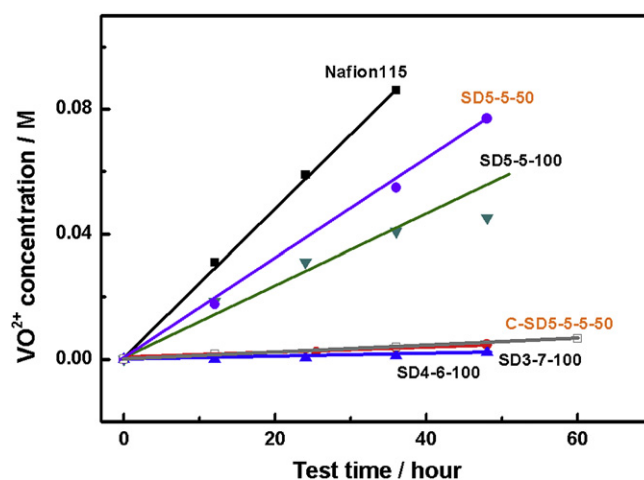

Fig. 3. TGA curves of membranes in acid form.

Fig. 5. VO^{2+} concentration in the right cell of the permeation measuring device with SDPEEK and Nafion 115 membranes.
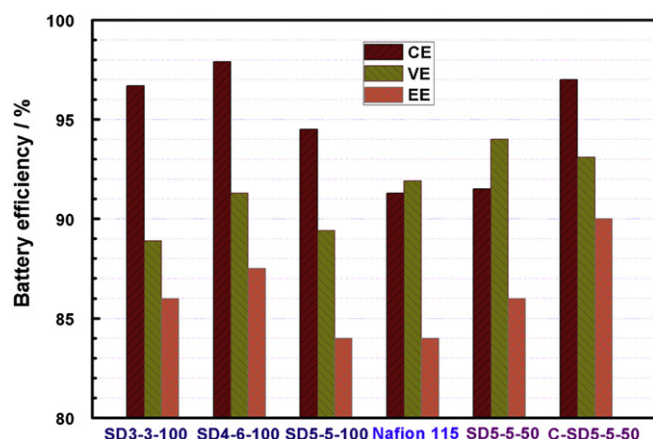
Fig. 6. VFB battery efficiency assembled with SDPEEK, Nafion 115 and crosslinked SDPEEK membranes under the charge–discharge current density of 50 mA cm^{-2}.

3.4. Single cell performance

The VFB single cell performance assembled with SDPEEK, Nafion 115 and crosslinked SDPEEK membranes is shown in Fig. 6. The columbic efficiency (CE) is defined as the ratio of a cell's discharge capacity (Q_{dis}) divided by its charge capacity (Q_{cha}) under certain charge–discharge conditions. The higher CE, indicating lower capacity loss, is mainly due to the lower rate of cross-mixed vanadium ions as well as the side reactions. The energy efficiency (EE) is defined as the ratio of a cell's discharge energy (E_{dis}) divided by its charge energy (E_{cha}). EE is a very important indicator, because it reflects the energy conversion efficiency of large scale energy storage devices. The voltage efficiency is defined as the ratio of average discharge voltage (V_{dis}) divided by its charge voltage (V_{cha}). Higher VE means lower battery resistance.

$$CE = \frac{Q_{dis}}{Q_{cha}} \times 100\% \qquad (5)$$

$$EE = \frac{E_{dis}}{E_{cha}} \times 100\% \qquad (6)$$

$$VE = \frac{V_{dis}}{V_{cha}} \times 100\% \qquad (7)$$
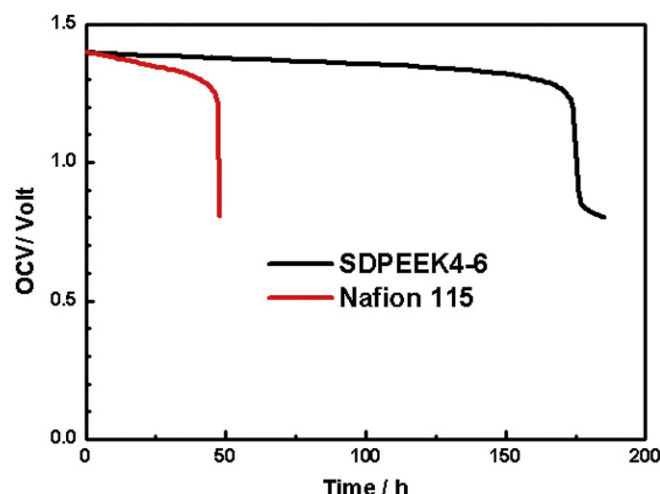

Fig. 8. OCV decay curves of the VFB cell assembled with SD4-6-100 and Nafion 115 membranes.

The SDPEEK membranes all exhibited higher CE than Nafion 115 membranes due to the much lower vanadium permeability. And with DS increasing from 0.6 to 1.0, the CE, VE and EE first increase then decrease. For example, the VFB cells assembled with SDPEEK membranes of DS 0.6, 0.8 and 1.0, show EE of 86%, 87.5% and 84% respectively. This is possibly due to the balance between ion selectivity and ion conductivity of the membranes. With increasing DS, the membranes show increased ion conductivity or lower membrane resistance. However, the membranes with high DS are prone to swell heavily in water, which would facilitate the cross-over of vanadium ions and lead to lower CE. In this case a balance between ion conductivity and vanadium permeation could be hopefully achieved in a VFB cell assembled with SDPEEK membranes.

In order to further increase the ion selectivity or decreasing swelling of SDPEEK membranes with high DS, the SD5-5-50 membrane was crosslinked via UV radiation. As a result of confined swelling, the crosslinked SDPEEK membrane (noted as C-SD5-5-50) shows much lower water uptake than uncrosslinked one (Table 1). And narrower or more disconnected ions pathway is correspondingly formed, rendering it more difficult for vanadium ions to permeate through the C-SD5-5-50 membranes. As expected,
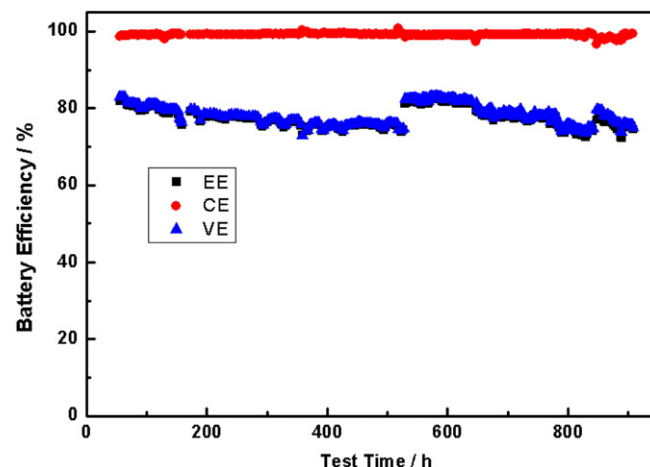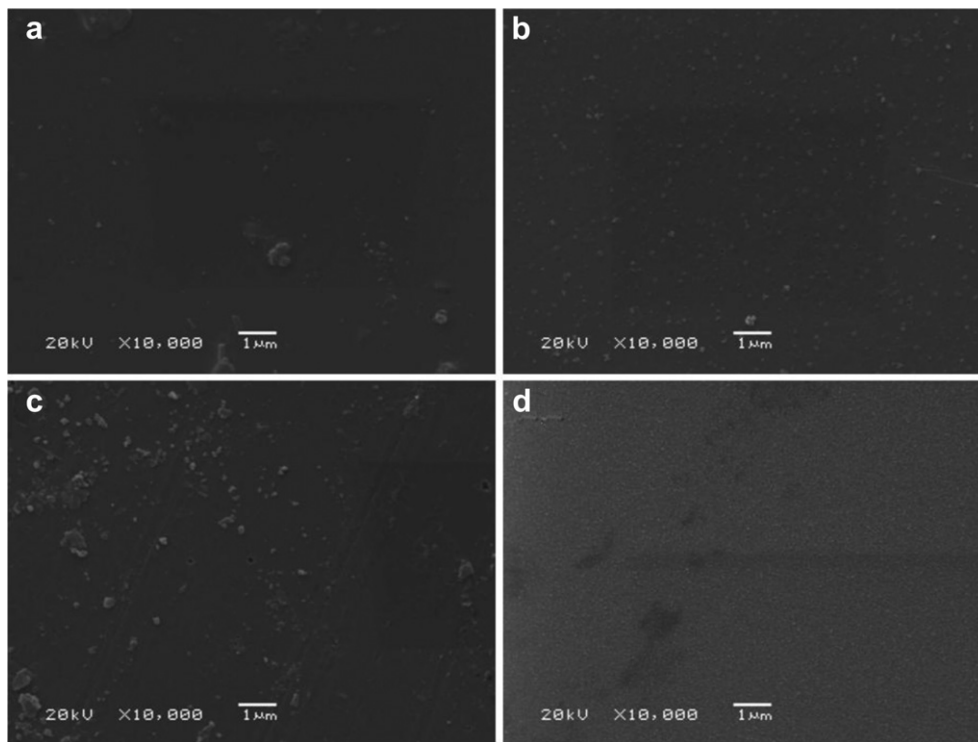

Fig. 7. Charge–discharge curves of the VRB cell assembled with SD5-5-50 and C-SD5-5-50 membranes.

Fig. 9. Charge–discharge cycling performance (80 mA cm^{-2}) of the cell with SD4-6-100.

Fig. 10. SEM of SD4-6-100 membrane: (a) initial surface (b) surface after life test (facing the anode) (c) surface after life test (facing the cathode) (d) cross-section after life test.

the vanadium ions permeability of C-SD5-5-50 in Table 1 is much lower than SD5-5-50 due to the improved ion selectivity caused by crosslinking.

Fig. 7 shows the VFB charge—discharge curves of SD5-5-50 and C-SD5-5-50 membranes. From the result, longer period of charge or discharge time means more capacity being charged or discharged in the batteries. In this system, the battery assembled with C-SD5-5-50 membrane shows less charge capacity and more discharge capacity than SD5-5-50 membrane during the charge—discharge process, due to the less capacity loss caused from vanadium ions crossover. Accordingly, the VFB cell assembled with the C-SD5-5-50 membrane achieves much higher CE than that of uncrosslinked SD5-5-50 membrane (Fig. 6).

As a result of higher CE and similar VE, most of the SDPEEK membranes exhibit much higher EE than Nafion 115 under the same test conditions. And the crosslinked C-SD5-5-50 membrane reached the EE of 90%, which is a fairly high value ever reported.

3.5. OCV test

Open circuit voltage (OCV) of the VFB single cell was monitored at room temperature after it was charged to 50% state of charge (SOC) and is presented in Fig. 8. As illustrated, the OCV value gradually decreases with storage time at first and rapidly drops to 0.8 V. It can be seen that the maintaining time of OCV above 1.0 V of the VFB single cell with SD4-6-100 is about 180 h, which is nearly three times longer than that of the VFB single cell assembled with pristine Nafion 115. This means that the self-discharge rate of the VFB cell assembled with SD4-6-100 is much slower than that assembled with Nafion 115, and the SD4-6-100 performs better than Nafion 115 in preventing vanadium ions crossover.

3.6. Stability tests

Chemical stability of SDPEEK membranes was further studied in VFB operation by continuous running for 900 h at a current density

of 80 mA cm^{-2} as shown in Fig. 9. The VFB cell showed stable performance, maintaining CE over 98% and EE around 80%, indicating the very good chemical stability of SDPEEK membranes. To note that, the jump in the middle of the test in Fig. 9 is mainly derived from the electrolytes recovery after very long time charge—discharge cycling test.

The membrane morphology before and after the VFB life test was detected via SEM (Fig. 10). Although the membrane shows dense and flat cross-sections, the surface of membranes after VFB life test is covered with very small dents and lumps compared with that of the initial membrane. The morphology of both surfaces of the membrane (facing the anode and the cathode) after VFB life test is similar, which is also similar with the study performed by Mai [14]. The reason for the morphology change of membrane surfaces is possibly due to the decreasing chemical stability in redox atmosphere or the physical squeeze of carbon felts and redox process near the membrane surface. Further study is undergoing in our lab to investigate the decomposition mechanism of carbon hydrogen membranes in VFB applications. And more researches are being executed to improve the physical and chemical stability of SDPEEK membranes, by ways of chemical modification and physical enhancement.

4. Conclusions

In this work, crosslinkable SDPEEK membranes with different DS were prepared and crosslinked as VFB separators for the first time. The physiochemical properties of SDPEEKs were studied in detail. The SDPEEK membranes showed higher ion selectivity and better VFB performance than Nafion 115 membrane under the same operating conditions. Performance of VFB cells assembled with SDPEEK membranes kept stable during 900-h running tests. And in order to further improve the ion selectivity of membranes with high DS or high swelling, UV crosslinking was carried out on the membrane with DS 100%. The results showed that UV crosslinking is an effective method to improve the ion selectivity of prepared

SDPEEK membranes, and further optimization on the crosslinking will be carried out in future.

Acknowledgements

References

[1] J.A. Turner, Science 285 (1999) 687–689.
[2] J.P. Barton, D.G. Infield, IEEE Trans. Energy Convers. 19 (2004) 441–448.
[3] I. Tsuda, K. Kurokawa, K. Nozaki, in: 1994 IEEE First World Conference on Photovoltaic Energy Conversion/Conference Record of the Twenty Fourth IEEE Photovoltaic Specialists Conference, 1994, vols. I and II, IEEE, New York, 1994, pp. 946–949.
[4] T. Shigematsu, T. Kumamoto, H. Deguchi, T. Hara, IEEE, Applications of a Vanadium Redox-flow Battery to Maintain Power Quality, IEEE, New York, 2002.
[5] A.H.W. Martha Schreiber, M. Harrer, R. Moser, in: Proceedings of the 8th International IEEE Conference on Intelligent Transportation Systems, Vienna, Austria, pp. 936–940.
[6] S.A. Lone, M.U.D. Mufti, IEEE, Integrating a Redox Flow Battery System with a Wind-diesel Power System, IEEE, New York, 2006.
[7] W. Zhang, M. Qiu, X. Lai, Power Syst. Technol. (Chinese) 32 (2008) 1–9.
[8] J. Li, The World of Inverters (Chinese) (2010) 65–67.
[9] C. Poncedeleon, A. Friasferrer, J. Gonzalezgarcia, D. Szanto, F. Walsh, J. Power Sources 160 (2006) 716–732.
[10] M. Skyllas-Kazacos, M.H. Chakrabarti, S.A. Hajimolana, F.S. Mjalli, M. Saleem, J. Electrochem. Soc. 158 (2011) R55–R79.
[11] P. Han, Y. Yue, Z. Liu, W. Xu, L. Zhang, H. Xu, S. Dong, G. Cui, Energy Environ. Sci. 4 (2011) 4710.
[12] D. Aaron, Z. Tang, A.B. Papandrew, T.A. Zawodzinski, J. Appl. Electrochem. 41 (2011) 1175–1182.
[13] T. Mohammadi, M. Skyllaskazacos, J. Membr. Sci. 98 (1995) 77–87.
[14] Z.S. Mai, H.M. Zhang, X.F. Li, C. Bi, H. Dai, J. Power Sources 196 (2011) 482–487.
[15] X. Li, H. Zhang, Z. Mai, H. Zhang, I. Vankelecom, Energy Environ. Sci. 4 (2011) 1147–1160.
[16] B. Schwenzer, J. Zhang, S. Kim, L. Li, J. Liu, Z. Yang, ChemSusChem 4 (2011) 1388–1406.
[17] P. Trogadas, E. Pinot, T.F. Fuller, Electrochem. Solid-State Lett. 15 (2012) A5.
[18] Z.S. Mai, H.M. Zhang, X.F. Li, S.H. Xiao, H.Z. Zhang, J. Power Sources 196 (2011) 5737–5741.
[19] H. Zhang, H. Zhang, X. Li, Z. Mai, J. Zhang, Energy Environ. Sci. 4 (2011) 1676–1679.
[20] H. Zhang, H. Zhang, X. Li, Z. Mai, W. Wei, Energy Environ. Sci. 5 (2012) 6299–6303.
[21] Y. Baek, N.S. Kwak, T.S. Hwang, Polym. Korea 35 (2011) 586–592.
[22] N.-S. Kwak, J. Koo, T. Hwang, Macromol. Res. 20 (2012) 205–211.
[23] C. Jia, J. Liu, C. Yan, J. Power Sources 203 (2012) 190–194.
[24] Q. Luo, H. Zhang, J. Chen, D. You, C. Sun, Y. Zhang, J. Membr. Sci. 325 (2008) 553–558.
[25] S. Zhang, C. Yin, D. Xing, D. Yang, X. Jian, J. Membr. Sci. 363 (2010) 243–249.
[26] L. Li, J. Chen, H. Lu, C. Jiang, S. Gao, X. Yang, X. Lian, X. Liu, R. Wang, Acta Chim. Sin. 67 (2009) 2785–2790.
[27] D. Chen, S. Wang, M. Xiao, D. Han, Y. Meng, J. Power Sources 195 (2010) 7701–7708.
[28] D. Chen, S. Wang, M. Xiao, Y. Meng, Energy Environ. Sci. 3 (2010) 622–628.
[29] D. Chen, S. Wang, M. Xiao, Y. Meng, J. Power Sources 195 (2010) 2089–2095.
[30] D. Chen, S. Wang, M. Xiao, D. Han, Y. Meng, Polymer 52 (2011) 5312–5319.
[31] S. Kim, J. Yan, B. Schwenzer, J. Zhang, L. Li, J. Liu, Z. Yang, M.A. Hickner, Electrochem. Commun. 13 (2011) 525.
[32] S. Kim, T.B. Tighe, B. Schwenzer, J. Yan, J. Zhang, J. Liu, Z. Yang, M.A. Hickner, J. Appl. Electrochem. 41 (2011) 1201–1213.
[33] S. Zhong, T. Fu, Z. Dou, C. Zhao, H. Na, J. Power Sources 162 (2006) 51–57.
[34] S. Zhong, C. Liu, H. Na, J. Membr. Sci. 326 (2009) 400–407.
[35] J. Rozière, D.J. Jones, Annu. Rev. Mater. Sci. 33 (2003) 503–555.